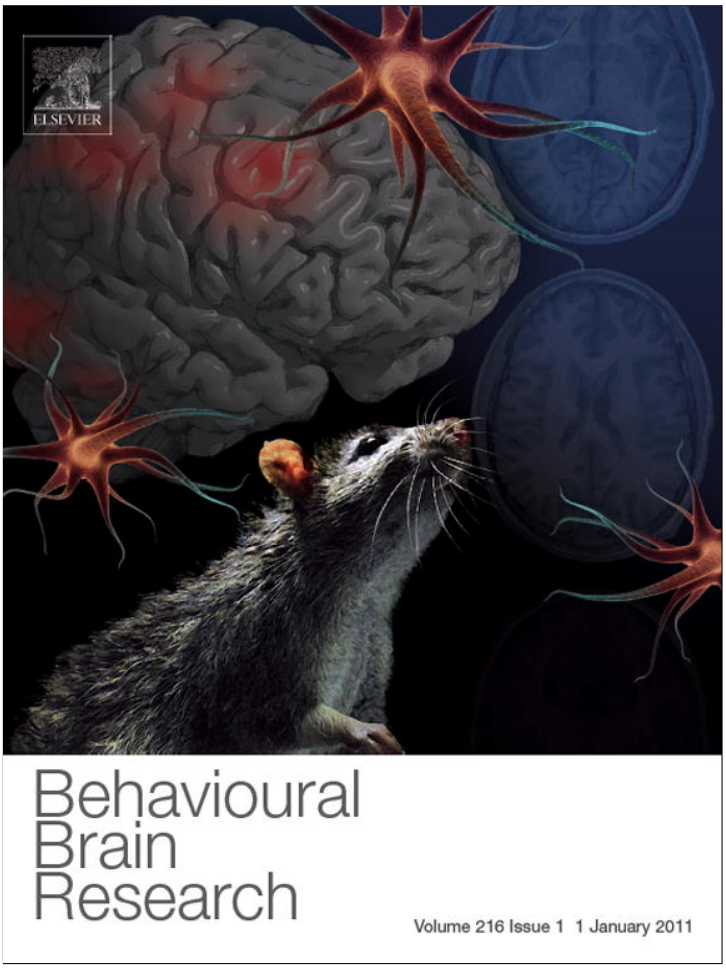

Behavioural Brain Research 216 (2011) 293–300

Contents lists available at ScienceDirect

Behavioural Brain Research

journal homepage: www.elsevier.com/locate/bbr

Research report

Manganese-enhanced magnetic resonance imaging (MEMRI) of rat brain after systemic administration of $MnCl_2$: Hippocampal signal enhancement without disruption of hippocampus-dependent behavior

Stewart J. Jackson[a,1], Rosalind Hussey[a,b,1], Maurits A. Jansen[c,d], Gavin D. Merrifield[c,d], Ian Marshall[c,d], Alasdair MacLullich[d,e,f], Joyce L.W. Yau[d,e], Tobias Bast[a,g,*]

[a] Centre for Cognitive and Neural Systems (CCNS), School of Biomedical Sciences, University of Edinburgh, Edinburgh, UK
[b] Department of Psychology and Trinity College Institute of Neuroscience, University of Dublin, Trinity College, Dublin 2, Ireland
[c] Medical Physics, School of Clinical Sciences and Community Health, University of Edinburgh, Edinburgh, UK
[d] Centre for Cardiovascular Sciences, School of Clinical Sciences and Community Health, University of Edinburgh, Edinburgh, UK
[e] Centre for Cognitive Ageing and Cognitive Epidemiology, University of Edinburgh, Edinburgh, UK
[f] Geriatric Medicine Unit, University of Edinburgh, Edinburgh, UK
[g] School of Psychology and Institute of Neuroscience, University of Nottingham, Nottingham, UK

ARTICLE INFO

Article history:
Received 24 March 2010
Received in revised form 1 August 2010
Accepted 8 August 2010
Available online 14 August 2010

Keywords:
Manganese
MRI
Hippocampus
Learning and memory
Delayed-matching-to-place task
Water maze
Rat

ABSTRACT

Manganese (Mn^{2+})-enhanced magnetic resonance (MR) imaging (MEMRI) in rodents offers unique opportunities for the longitudinal study of hippocampal structure and function in parallel with cognitive testing. However, Mn^{2+} is a potent toxin and there is evidence that it can interfere with neuronal function. Thus, apart from causing adverse peripheral side effects, Mn^{2+} may disrupt the function of brain areas where it accumulates to produce signal enhancement and, thereby, Mn^{2+} administration may confound cognitive testing. Here, we examined in male adult Lister hooded rats if a moderate systemic dose of $MnCl_2$ (200 μmol/kg; two intraperitoneal injections of 100 μmol/kg separated by 1 h) that produces hippocampal MR signal enhancement would disrupt hippocampal function. To this end, we used a delayed-matching-to-place (DMP) watermaze task, which requires rapid allocentric place learning and is highly sensitive to interference with hippocampal function. Tested on the DMP task 1 h and 24 h after $MnCl_2$ injection, rats did not show any impairment in indices of memory performance (latencies, search preference) or any sensorimotor effects. However, $MnCl_2$ injection caused acute peripheral effects (severe ataxia and erythema, i.e. redness of paws, ears, and nose) which subsided over 30 min. Additionally, rats injected with $MnCl_2$ showed reduced weight 1 day after injection and failed to reach the normal weight–growth curve of control rats within the 16 days monitored. Our results indicate that 200 μmol/kg $MnCl_2$ produces hippocampal MR signal enhancement without disrupting hippocampus-dependent behavior on a rapid place learning task, even though attention must be paid to peripheral side effects.

1. Introduction

Following systemic administration, manganese (Mn^{2+}) enters the brain and enhances the T1-weighted magnetic resonance (MR) signal in brain regions where it accumulates (by reducing the T1 relaxation times of water protons) and, thereby, facilitates high-resolution MR imaging (MRI) of these regions [1]. Manganese accumulation is activity dependent, as the cation can enter neurons via voltage-gated Ca^{2+} channels, and, therefore, Mn^{2+}-enhanced MRI (MEMRI) can be used to image regional brain activation during an animal's behavior in the hours following Mn^{2+} administration [2–10]. In the rodent brain, the hippocampus, which combines specific memory mechanisms with links to diverse behavioral control functions [11,12], is among the sites showing particularly strong Mn^{2+} accumulation [1,9,13,14]. Thus, MEMRI offers intriguing opportunities for the high-resolution mapping of hippocampal structure and function in parallel to cognitive testing in rodents. Due to its relatively non-invasive nature, MEMRI may be particularly suitable for longitudinal studies in rodent models of disorders in which hippocampal dysfunction has been implicated, such as cognitive aging, Alzheimer's disease, and schizophrenia (e.g., [15–19]).

* Corresponding author at: School of Psychology, University of Nottingham, University Park, Nottingham NG7 2RD, UK. Tel.: +44 115 84 67438.
E-mail address: tobias.bast@nottingham.ac.uk (T. Bast).
[1] Contributed equally.

0166-4328/$ – see front matter © 2010 Elsevier B.V. All rights reserved.
doi:10.1016/j.bbr.2010.08.007

A key challenge for MEMRI is that Mn^{2+} is a potent toxin that can have adverse side effects on peripheral organs and the brain when the very low normal concentrations of this essential trace metal are exceeded [20]. Manganese doses used for MEMRI (ranging from approximately 100 to 900 μmol/kg) have typically not been reported to produce severe adverse effects, even though skin damage at the injection side, depressed behavioral activity, and weight loss have been reported [1,6,14,21]. However, in vitro studies indicate that supra-physiological levels of Mn^{2+} interfere with cellular mechanisms critical for synaptic transmission and plasticity, including NMDA receptor-mediated mechanisms [22,23]. Hence, Mn^{2+} may disrupt the neuro-behavioral functions of brain areas where it accumulates, such as the hippocampus; thereby, cognitive testing in conjunction with MEMRI may be confounded. Previous studies have carefully investigated the effects of systemic Mn^{2+} administration on retinal functions and not found adverse effects at a moderate dose (anhydrous $MnCl_2$: 44 mg/kg; 350 μmol/kg, intraperitoneal (i.p.)) [24,25]. However, the possibility that systemically applied Mn^{2+}, at doses suitable for MEMRI, may interfere with neuro-behavioral functions of other brain regions, including the hippocampus, has, until very recently [14], received little attention.

In this study, we examined in Lister hooded rats if a systemic injection of manganese chloride ($MnCl_2{\cdot}4H_2O$: 200 μmol/kg, intraperitoneal (i.p.)) that produces pronounced hippocampal MR signal enhancement (see Fig. 1) would disrupt hippocampal function. For this purpose, we used the delayed-matching-to-place (DMP) watermaze task, which requires behavior based on rapid, one-trial, allocentric place learning and is highly sensitive to interference with hippocampal function [26–29]. We also monitored the rats for signs of peripheral non-specific adverse side effects of Mn^{2+}.

2. Materials and methods

2.1. Animals

Adult male Lister hooded rats (Charles River, UK) were used. The main experiment, involving watermaze testing, used 24 rats (average weight of 300 g, ranging from 288 to 316 g, and ca. 10 weeks old on the first day of watermaze training; average weight of 358 g, ranging from 334 to 396 g, and ca. 12 weeks old on the day of $MnCl_2$ or control injection). Four rats (two rats weighing 365 and 370 g and 12 weeks old, one rat 450 g and 18 weeks old, and one rat 563 g and 22 weeks old on the day of $MnCl_2$ injection), were used to demonstrate that the $MnCl_2$ dose used in the main experiment produced hippocampal MR signal enhancement. Rats were housed in groups of four, and were given *ad libitum* access to food and water. They were kept on a 12–h light/dark cycle (lights on at 7:00 a.m.) in a temperature (20–23 °C)- and humidity (40–55%)-controlled environment. Experiments were only performed during light hours. Before the start of experiments, all rats were habituated to handling by the experimenters. Animal experiments were carried out in accordance with the "Principles of Laboratory Animal Care" (NIH Publication No. 86-23, revised 1985) and with UK Home Office regulations.

2.2. Manganese chloride injections

Hydrated manganese chloride ($MnCl_2{\cdot}4H_2O$, Sigma–Ulrich, UK) was dissolved in a 400 mM bicine (di(hydroxyethyl)glycine, Sigma–Ulrich, UK) buffer (pH, 7.4) at a concentration of 100 μmol/ml (20 mg/ml) similar to previous studies [1]. Rats were administered a total dose of 200 μmol/kg (i.e. 40 mg/kg $MnCl_2{\cdot}4H_2O$), in the form of two i.p. injections of 1 ml/kg $MnCl_2$ (100 μmol/ml) separated by 1 h. The total dose was injected in two steps to reduce acute peripheral Mn^{2+} overexposure (also compare [21]). Based on veterinary advice and in order to minimize any pain due to acute Mn^{2+} overexposure, rats were injected subcutaneously with the analgesic carprofen at a dose of 4 mg/kg and an injection volume of 0.8 ml/kg 1 h before $MnCl_2$ injection (Rimadyl, Pfizer, UK, containing 50 mg/ml carprofen, was dissolved in 0.9% saline to create a solution of 5 mg/ml). As control, rats received carprofen injection, followed 1 h later by two injections of 1 ml/kg of 400 mM bicine buffer.

The dose of 200 μmol/kg $MnCl_2$ (40 mg/kg $MnCl_2{\cdot}4H_2O$) was based on pilot dosing studies in our Lister hooded rats, in which we found that higher doses resulted in clearer MR signal enhancement, but also in fatalities, whereas lower doses failed to result in clear hippocampal MR signal enhancement. More specifically, one rat died after injection of 500 μmol/kg (99 mg/kg of $MnCl_2{\cdot}4H_2O$; one rat injected) and another rat died after injection of 300 μmol/kg (59 mg/kg of $MnCl_2{\cdot}4H_2O$; two injections of 150 μmol/kg, 1 h apart; two rats injected). It should be noted that previous studies in Sprague–Dawley rats have not reported mortality at these or even higher doses [1,6,14,21,24,25], indicating strain differences. Lower doses of $MnCl_2$, 150 and 120 μmol/kg (i.e. 30 mg/kg and 24 mg/kg of $MnCl_2{\cdot}4H_2O$; one and four rats injected, respectively), were also tested, but the level of signal enhancement 24 h after the last injection was not as clear as at the higher doses. In our pilot studies, we also found that $MnCl_2$, at least at the dose of 150 μmol/kg, does not affect the stress response of the rats: corticosterone levels measured by radioimmunoassay modified for microtitre plate scintillation proximity assay in blood samples [30] did not differ before and after $MnCl_2$ injection (125 ± 35.3 nM in a morning basal blood sample taken by venesection 24 h after i.p. vehicle injection and 120 ± 20.3 nM in another blood sample taken, 2 weeks later, 24 h after 150 μmol/kg $MnCl_2$; $n = 3$).

Within the first 1 h after injection, the rats' behavior was carefully monitored (acute peripheral side effect typically subsided within 30 min, see Section 3.3). On the subsequent days, rats were checked daily, including inspection of the injection site, and weights were recorded for 16 days.

2.3. Magnetic resonance imaging

In order to confirm that our systemic $MnCl_2$ injection (200 μmol/kg) results in substantial hippocampal Mn^{2+} accumulation, we obtained T1-weighted MR brain scans from four rats before (1–2 weeks) and 24 h after $MnCl_2$ injection, at which time Mn^{2+}-induced signal enhancement should have reached a stable asymptotic level [13,14].

All MRI experiments were performed using a 7-T horizontal bore NMR spectrometer (Varian, Palo Alto, CA, USA), equipped with a high-performance gradient insert (12-cm inner diameter, maximum gradient strength 400 mT/m). The rat was anaesthetized with 1.5–2% isoflurane in oxygen (1 L/min), placed in a cradle (Rapid Biomedical GmbH, Rimpar, Germany), and the skull was fixed with plastic ear bars. Rectal temperature and respiration rate were monitored throughout the experiments, and body temperature was maintained at 37.0 ± 0.5 °C with a heat fan. A birdcage coil (72-mm diameter) was used for radio frequency transmission and a dedicated brain coil (2-channel phased array, Rapid Biomedical GmbH, Rimpar, Germany) for signal reception. To allow comparison, the same receiver gain setting was used for the scans before and after $MnCl_2$ injection. Twenty-four contiguous coronal T1-weighted fast spin echo images (echo train length 4) of 0.5 mm slice thickness were collected with the following parameters: repetition time (TR) = 1000 ms; effective echo time = 9.64 ms; field of view = 25.6 mm × 25.6 mm; matrix = 256 × 256 (i.e. 100 μm in-plane resolution); 30 signal averages; total scan time was 32 min. We chose a TR of 1000 ms based on two considerations: first, according to published estimations, T1-weighted signal enhancement induced by Mn^{2+} tissue concentrations of 5–50 μM is maximal at TRs around 1000 ms, with the optimal TR decreasing with increasing Mn^{2+} concentrations [1]. It is reasonable to expect tissue concentrations of this range in forebrain areas following systemic application of low to moderate Mn^{2+} doses, such as 200 μmol/kg. Indeed, hippocampal Mn^{2+} concentrations were measured to be approximately 40 μM 24 h after two i.p. injections of 200 μmol/kg, 24 h apart, in Sprague–Dawley rats [31]. Second, as compared to shorter TRs, a TR of 1000 ms enabled us to image a larger part of the brain in a given scanning time. In one experiment, we compared Mn^{2+}-induced hippocampal signal enhancement at a TR of 1000 ms with enhancement at the shorter TR of 300 ms without finding striking differences; if at all, hippocampal enhancement was stronger at a TR of 1000 ms (data not shown).

Additional scans of a cylindrical vial, approximately the size of a rat's head and containing saline with GdDOTA (gadolinium tetraaza-cyclododecane-tetraacetic acid), were acquired to be used for correcting the brain images for signal intensity changes as a function of distance from the surface coil (compare [4]). The scans of the cylindrical phantoms were acquired with the same receiver gain setting and with the same position parameters as the respective brain scans with an acquisition matrix of 64 × 64 and 10 signal averages. Finally, to test for day-to-day stability of our MR system, a small vial containing Vaseline was placed on the surface coil above the rat's head, always in the same position, during the six scans of the last three rats. Signal intensities obtained from this external standard showed minimal variation across scans (maximum change <3%).

2.3.1. Assessment of manganese-induced signal enhancement

On coronal images, regions of interest (ROIs) were manually placed within the dorsal hippocampus and in the pituitary (see Fig. 1, left). To correct for signal-intensity gradients due to surface coil use, brain images were divided by the coil intensity profile obtained from the scans of the cylindrical phantom. Subsequently, the corrected mean signal intensity of all voxels in the respective ROIs, averaged for both hemispheres, was calculated. To confirm significant Mn^{2+}-induced enhancement, mean signal intensities before and after $MnCl_2$ injection were compared using one-tailed paired *t*-tests (significance level $p < 0.05$). The percentage of enhancement in each ROI was calculated as: 100% × (corrected signal intensity after Mn^{2+} − corrected baseline signal intensity)/corrected baseline signal intensity.

2.4. Watermaze testing

2.4.1. Apparatus

A circular 2-m diameter open-field watermaze was filled with water at 25 ± 1 °C. The pool was located in a well lit, rectangular, and white-walled room. Prominent cues, visible from the water surface, were positioned at variable distances from the pool, so as to be used by the rats for efficient allocentric orientation. Once rats

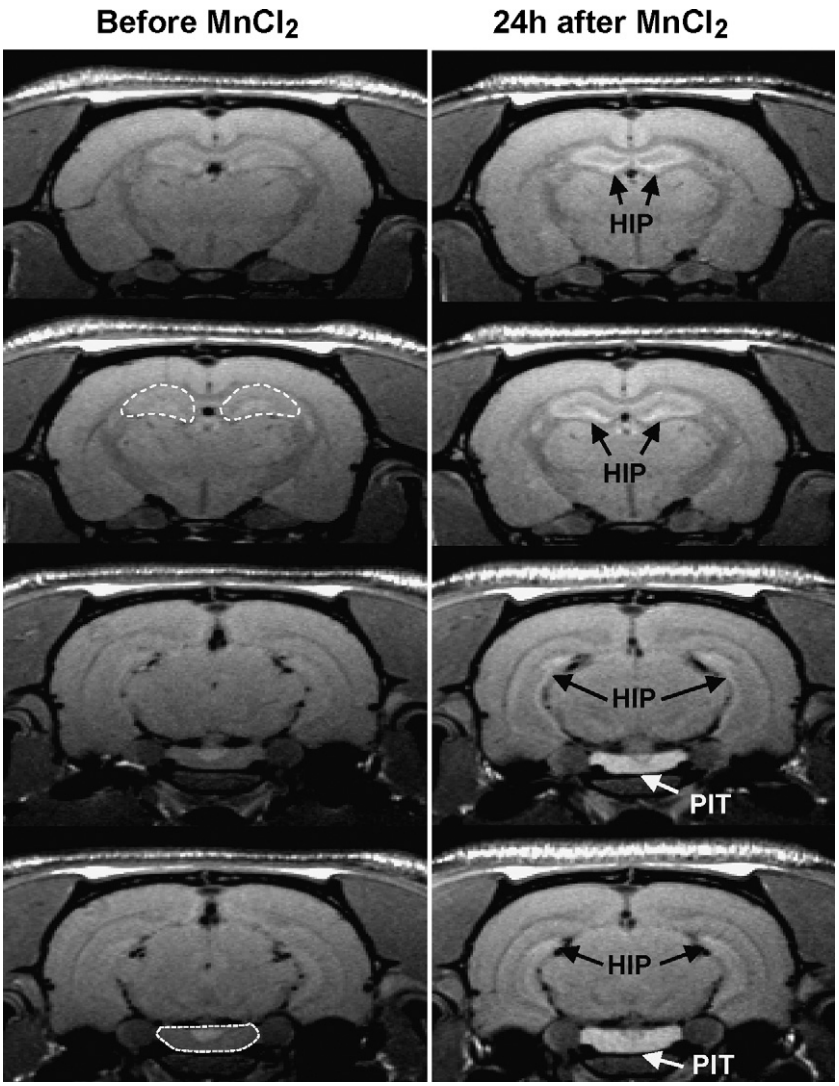

Fig. 1. Manganese-enhanced brain magnetic resonance imaging following i.p. injection of 200 μmol/kg $MnCl_2$. Coronal T1-weighted brain images of one rat before (left) and 24 h after (right) a 200 μmol/kg injection of $MnCl_2 \cdot 4H_2O$. Images are arranged from anterior at the top to posterior at the bottom and were 1.5 mm apart. Note the pronounced signal enhancement in principal cell layers of the hippocampus (HIP) and in the pituitary (PIT) 24 h after injection of $MnCl_2$. The regions of interest (ROIs) used for quantitative analysis of Mn^{2+}-induced signal enhancement in hippocampus and pituitary are indicated by the stippled white outlines on the brain images on the left.

had been placed in the water, their sole route of escape was via a single escape platform, which was 12 cm in diameter. The platform was hidden from the animals' sight 1–2 cm below the surface of the water, which was made opaque by addition of 200 ml of latex. We used the 'Atlantis Platform' [32], which can be held >30 cm below the water surface (inaccessible for the rats) by a computer-controlled electromagnet for a prearranged time, before rising to its normal position. This enables rewarded probe trials during which the rats' search preference is first monitored for 60 s, and the platform is then made available to reinforce spatially focused searching.

The rats' behavior was monitored by an overhead video camera attached to a video recorder and computer in an adjoining control room. Watermaze software (Actimetrics, Wilmette, IL) was used to digitize the path taken by the animal and assisted collection of the following measures: escape latency, swim speed, and search preference as indicated by '% time spent in the correct zone' (compare Section 2.4.2).

2.4.2. Delayed-matching-to-place (DMP) task

On the DMP task [26], rats receive 4 trials a day. The platform is hidden in a novel location on trial 1 of each day and then remains in this place for trials 2–4, on which rats can use rapidly-encoded place memory to reach the escape platform efficiently (compare Fig. 2A). All four start positions are used daily in an arbitrary sequence, to discourage egocentric strategies. Analysis focuses on trial 2 of each day, on which performance relies on place memory encoded within a single trial, while trials 3 and 4 are run to reinforce the win-stay rule of the task. Whereas the original DMP task relies exclusively on escape latencies to measure performance [26], we used a novel task modification [29] where trial 2 is occasionally run as rewarded probe trial. On rewarded probe trials, the platform is not made accessible for the rat until after 60 s, enabling the measurement of the rats' search preference for the zone containing the platform location (see Section 2.4.3).

Each trial began with the rat being placed in the pool facing the side wall at one of four arbitrary cardinal points around the watermaze (North (N), East (E), South (S) and West (W)). Rats had a maximum of 120 s to search for the hidden escape platform. Rats failing to locate the platform after 2 min were guided to the platform by the experimenter. Once rats had reached the platform they were given 30 s to remain on the platform and encode its spatial location using the surrounding visual cues. On each day, the rat was released from all four cardinal points, the sequence of which was changed between days. The center of the escape platform was either located on an inner ring (0.8 m diameter) or outer ring (1.4 m) concentric with the pool. Rats were tested with a novel location each day.

2.4.3. Performance measures: latencies and search preference

Latencies to reach the platform perimeter (or 120 s as maximal trial duration) were recorded for all trials; a steep latency reduction from trial 1 to 2 indicates rapid one-trial place learning. In addition, search preference for the vicinity of the platform location when trial 2 was run as probe trial was used to measure rapid place learning that had occurred during trial 1; search preference is less chance-dependent than latencies and a more reliable measure of hippocampus-dependent place memory [29].

To measure search preference, eight 40-cm diameter 'virtual' zones, one of which (the 'correct zone') was concentric with the platform location, were defined on the inner and outer ring of the pool, so that the zones were non-overlapping, evenly spaced, and symmetrically arranged (see Fig. 2B). The time spent in each of these eight zones during the 60-s probe trial was determined automatically using

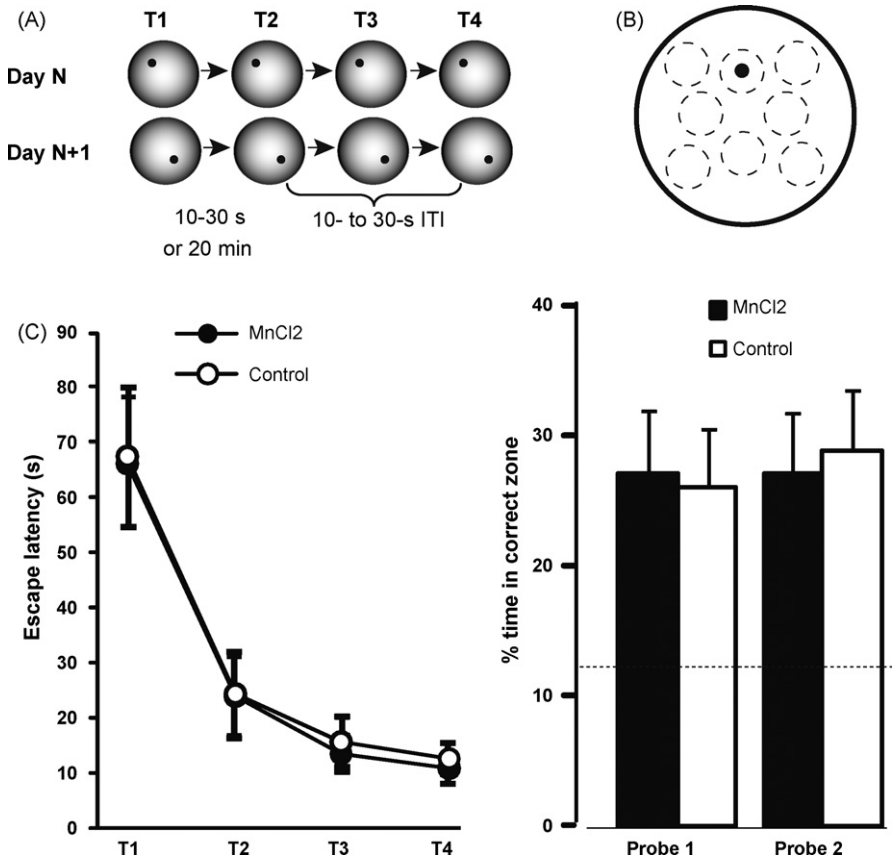

Fig. 2. The delayed-matching-to-place task in the watermaze and matched pre-training performance measures in the prospective $MnCl_2$- and control-injection groups. (A) Rats had four daily trials (T1–T4) in the watermaze. The location of the hidden escape platform (black dot) was constant within a day, but the platform was moved to a novel location at the beginning of each day. Thus, rapid place learning during T1 of each day enabled efficient performance during T2 and the subsequent trials. The retention delay between T1 and T2 was 10–30 s during the first 2 days of pre-training and 20 min throughout the rest of the study, whereas all other inter-trial intervals (ITI) within a day were always 10–30 s. Trial 2 was occasionally run as probe with the platform not coming up until after 60 s, during which time the search preference for the area containing the platform location could be measured. (B) Zone analysis of search preference on probes: eight 40-cm-diameter zones (stippled circles) were defined within the 2-m diameter of the watermaze, including the correct zone, which was concentric with the location of the platform (12-cm diameter; black dot) on trial 1 of the day. The zones were non-overlapping, evenly spaced, and symmetrically arranged. The time rats spent in the different zones during the 60-s probe trial was measured, and the percentage of time spent in the correct zone was calculated as: (time in the correct zone/time in all eight zones) × 100%. By chance, i.e. during random swimming, this value should be 12.5%, whereas higher values indicate a search preference for the correct zone based on one-trial place learning. (C) Matched pre-training performance in the prospective injection groups ($MnCl_2$ or control): latencies (mean ± SEM) to find the hidden escape platform on T1–T4 averaged for the 9 days of pre-training (left) and search preferences (mean + SEM) for the correct zone when T2 was run as probe on days 6 and 8 of pre-training (probes 1 and 2, respectively). Note the sharp reduction in latencies from T1 to T2, as well as the highly above-chance search preference for the correct zones on probe trials; both of these effects reflect rapid one-trial place learning of the daily novel platform location. Stippled line indicates chance-level search time in the correct zone (12.5%).

the Watermaze software. From these measures the '% of time spent in the correct zone' was calculated as: (time in 'correct zone'/time in all eight zones) × 100%. By chance, i.e. during random swimming, this value should be: 100%/8 = 12.5%, while higher values indicate a search preference for the 'correct zone'.

Both latency and search preference measure are highly sensitive to interference with hippocampal function. For example, in previous studies from our laboratory, complete neurotoxic lesions of the hippocampus completely prevented the latency (or path-length) decreases, so-called 'savings', that are usually observed between trials 1 and 2 [26,29]. Such lesions also completely prevented the development of any search preference for the correct zone on trial 2 [29]. Partial hippocampal lesions removing the intermediate 60% of hippocampal volume and sparing 20% of total hippocampal volume at both dorsal and ventral tip of the hippocampus [29] had similar effects. Moreover, antagonism of hippocampal NMDA receptors by intracerebral infusion of AP5 led to a ca. 50% reduction in latency decreases ('savings') from trial 1 to 2, if the retention delay between the trials exceeded a few seconds [26].

2.4.4. Pre-training on the DMP task (days 1–9)

Before testing the effects of $MnCl_2$ injections, rats were pre-trained on the DMP task for 9 days to reach asymptotic performance levels (there was one day without training between pre-training days 1 and 2 and two days without training between days 3 and 4 and days 8 and 9). Probe trials were run on trial 2 of days 6 and 8. For the first 2 days, the time between each of the four trials was as short as possible, i.e. 10–30 s, for convenience. Starting with day 3, trials 1 and 2 were 20 min apart, while the delay was kept at 10–30 s between the other trials. Using the longer retention delay between trials 1 and 2 renders the DMP task sensitive to disruption of hippocampal plasticity mechanisms, including NMDA receptor-mediated mechanisms, that are not required at shorter delays [26]. Based on the performance measures during pre-training, rats were divided into two performance-matched groups to study the effects of $MnCl_2$ and control injections. The intended group sizes ($n = 12$) were similar to those in previous experiments from our laboratory ($n = 9$–12) that assessed the effects of hippocampal lesions and found highly significant differences compared to control rats ($p < 0.005$) in search preferences (main effect of group) and/or latency/path-length measures (group × trial interaction) [26,29]. Moreover, the effects of partial and complete hippocampal lesions on search preference that are described above (Section 2.4.3) correspond to effect sizes of Cohen's $d = 1.0$–1.4, and with group sizes of $n = 12$ the statistical power to detect such effects is roughly 0.8–0.95 (estimated using G*Power 3 [33]).

2.4.5. Testing on the DMP task following $MnCl_2$ injections (days 10 and 11)

Rats received $MnCl_2$ or control injections on day 10. Both injection groups were then tested on the DMP task 1–2 h later and 24 h later (i.e. on day 11). At both time points, rats were given four trials, with a 20-min retention delay between trials 1 and 2 and trial 2 run as a probe trial. Start positions and platform locations for the two injection groups were counterbalanced. Previous studies of the time course of Mn^{2+} uptake in the rat brain suggest that 1–2 h after systemic Mn^{2+} injection, Mn^{2+} concentrations in the hippocampus are still relatively low and not much different from surrounding tissue, whereas after 24 h stable asymptotic levels of Mn^{2+}-induced MR signal enhancement are present in the hippocampus [13,14]. Our own MRI experiments also confirmed that, 24 h after $MnCl_2$ injection, there is pronounced hippocampal signal enhancement (Section 3.1 and Fig. 1). Thus, testing 1–2 h after injection preferentially assessed peripheral and extra-hippocampal

effects of Mn^{2+}, whereas testing at 24 h should have revealed any deficits due to hippocampal Mn^{2+} accumulation.

2.5. Statistical analysis

The watermaze data were analyzed using analysis of variance (ANOVA), with group as between-subjects factor and trials as within-subjects factor. Significant effects indicated by the ANOVA were further analyzed using Fisher's least-significant difference test. Two-tailed one-sample *t*-tests were performed when comparing zone preference to chance. To assess effects of $MnCl_2$ injection on rat weights, individual weights were normalized to the pre-injection weight on the morning of the injection day, and analyzed using ANOVA with group as between-subjects factor and day as within-subjects factor. A significance level of $p = 0.05$ was accepted for all comparisons. Data are presented as mean ± SEM.

3. Results

3.1. Manganese-enhanced magnetic resonance imaging

Injection of $MnCl_2$ resulted in enhanced T1-weighted signal in brain scans obtained 24 h after injection. Consistent with previous studies [e.g., 1,9,13,14], Mn^{2+}-induced signal enhancement is highly heterogeneous across the brain, with some structures, including the hippocampus, showing particularly pronounced enhancement (Fig. 1). Quantitative analysis (Section 2.3.1) revealed that 24 h following $MnCl_2$ injection, the T1-weighted MR signal in the ROIs placed within hippocampus and pituitary (see Fig. 1, left) was significantly enhanced (one-tailed paired *t*-tests, $p < 0.05$). The signal enhancement (mean ± SEM) was 20.7 ± 8.9% in the hippocampus and 109.9 ± 15.7% in the pituitary.

3.2. DMP task acquisition and matching

Rats showed successful task acquisition, similar to previous studies [26,28,29]. Rats typically showed the highest latencies on trial 1 of a day, reflecting searching for the novel platform position, and strikingly reduced latencies from trial 2 onwards, reflecting more efficient navigation based on rapid one-trial place learning (main effect of trial on escape latencies across the nine days of pre-training: $F_{(3, 69)} = 340.7$, $p < 0.0001$; trial 1 vs. trial 2: Fisher's least-significant difference test, $p < 0.0001$) (data not shown). Results from the probe trials on days 6 and 8 revealed that rats spent significantly more time in the correct zone (27% and 28%) than expected based on chance ($t(23) > 4.0$, $p < 0.001$).

Two matched groups were created based on the pre-training performance measures. One rat that showed highly anomalous probe-trial performance on both days 6 and 8 (0% time spent in the correct zone) was excluded before matching to prevent confounding results during testing. The remaining 23 rats were divided into two groups which were matched according to latency and search preference measures (Fig. 2C). Twelve rats received $MnCl_2$ injections and 11 received control injections (see Section 2.2).

3.3. Acute effects of $MnCl_2$ injection: ataxia and erythema

Immediately after the first $MnCl_2$ injection (100 μmol/kg), paws, noses and ears of the rats became erythematous (showed "flushing"). The rats also became severely ataxic and apparently unable to control their limbs. There was some variability in the reaction to $MnCl_2$ injections, with different rats showing these acute side effects with different severities and recovery times. However, all rats returned to normal activity after approximately 30–45 min. The effects of the second injection (another 100 μmol/kg to complete the total dose of 200 μmol/kg) were similar to the first injection, but appeared overall less pronounced. At the time of watermaze testing, i.e. 1–2 h following the second $MnCl_2$ injection, acute side effects had completely subsided in all rats. In the group of rats receiving control injections, no rat demonstrated any abnormalities.

3.4. Watermaze testing

3.4.1. Swimming and platform behavior

Swimming and platform behavior in the watermaze is very sensitive to any sensorimotor impairment [34–36]. We carefully monitored such behavior, but did not observe any abnormalities in any of the rats. In addition, we compared swim speeds in the two injection groups. Across the two probe trials, average swim speeds (mean ± SEM) were 23.31 ± 0.60 cm/s in rats that had received $MnCl_2$ injections and 23.04 ± 0.97 cm/s in control rats. ANOVA of swim speeds across the two probe trials neither revealed a main effect of group ($F_{(1, 21)} = 0.1$), nor a main effect of probe trial ($F_{(1, 21)} = 2.5$, $p > 0.1$) or an interaction of probe trial and group ($F_{(1, 21)} = 0.2$). Thus, observations during watermaze testing did not reveal any sensorimotor side effects either 1–2 h or 24 h following $MnCl_2$ injection.

3.4.2. Escape latencies

Escape latencies did not indicate any performance impairment due to $MnCl_2$ injection. Both 1–2 h and 24 h after injection, $MnCl_2$-injected rats showed similar latencies to control rats and, importantly, a pronounced latency reduction from trial 1 to 2, indicating intact one-trial place learning (Fig. 3A). Statistical analysis of the latencies from the DMP tests 1–2 h and 24 h after injection only revealed main effects of trial ($F_{(3, 63)} = 19.3$, $p < 0.0001$, and $F_{(3, 63)} = 10.7$, $p < 0.0001$, respectively), with latencies on trial 1 significantly longer than on trial 2 (Fisher's least-significant difference test, $p < 0.0001$ and $p < 0.025$, respectively), but no main effects of group ($F_{(1, 21)} = 0.2$ and $F_{(1, 21)} = 3.6$, $p > 0.07$, respectively), nor interactions between trial and group ($F_{(3, 63)} = 0.9$ and $F_{(3, 63)} = 1.4$, $p > 0.2$, respectively).

3.4.3. Search preference on trial 2

Search preference data from the probes on trial 2 of DMP testing 1–2 h and 24 h after injection, did not show any difference between $MnCl_2$ and control rats. At both intervals after the injection, both groups showed comparable, above-chance, search preference for the correct zone (Fig. 3B). Statistical analysis of probe-trial search preferences on the DMP tests 1–2 h and 24 h after injection did not reveal any significant difference between groups ($F_{(1, 21)} = 2.2$, $p > 0.15$, and $F_{(1, 21)} = 0.1$, respectively), and in both groups search preferences for the correct zone were significantly higher than chance (all $t > 2.2$, $p < 0.05$).

3.5. Injection sites and rat weights

All rats were carefully monitored for 16 days following injections. During this period none of them presented any obvious abnormal behavior. Inspection of the injection sites revealed that six rats, five of which had been injected with $MnCl_2$, had small lumps at the site of injection, consistent with the report of 'occasional abdominal indurations' reported after i.p. injection of 3×60 mg/kg of $MnCl_2 \cdot 4H_2O$ in Sprague–Dawley rats [21] and indicating that $MnCl_2$ may contribute to skin irritation around the injection site. In our study, any abnormalities around the injection site had disappeared in all rats by day 13 after the injection.

Furthermore, rats injected with $MnCl_2$ showed reduced weight on the day following injection. Their weight–growth curve converged with that of the control injection group within the 16 days monitored, even though control weight levels were not completely reached (Fig. 4). These impressions were supported, by a main effect of group on normalized rat weights across the pre-injection day

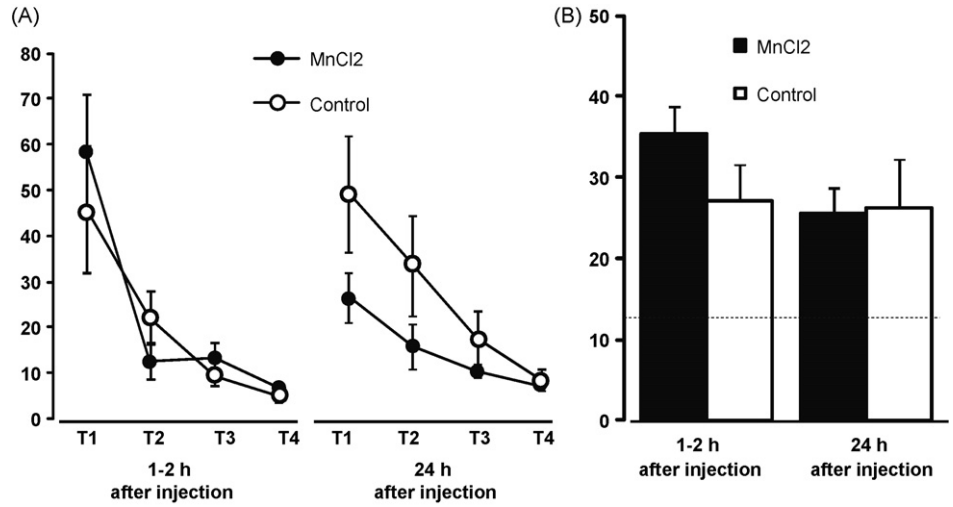

Fig. 3. Intact performance on the delayed-matching-to-place task following injection of $MnCl_2$. (A) Latencies (mean ± SEM) to find the hidden escape platform on trials 1–4 (T1–T4) and (B) search preference (mean + SEM) for the correct zone on the probe trials (trials 2) during DMP testing 1–2 h and 24 h after $MnCl_2$ or control injections. Stippled line indicates chance-level search time in the correct zone (12.5%).

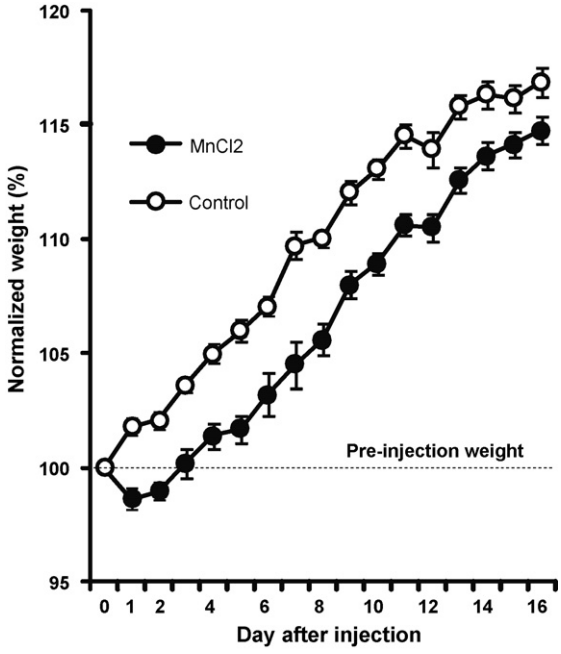

Fig. 4. Reduced weight in rats injected with $MnCl_2$, as compared to the control-injected group. Weights are depicted from the day of injection until day 16 after $MnCl_2$ or control injections. All weights are normalized to values on the morning of the injection day (pre-injection weight, 100%). * Significant main effect of group across days and interaction group × days, reflecting initial weight loss in the $MnCl_2$ group and subsequent convergence with the control weight-growth curve.

and the 16 days following injection ($F_{(1, 21)} = 28.3$, $p < 0.0001$), and an interaction between group and days ($F_{(16, 336)} = 5.3$, $p < 0.0001$).

4. Discussion

We showed that a dose of 200 μmol/kg $MnCl_2$ results in pronounced hippocampal MR signal enhancement in Lister hooded rats without interfering with the behavioral function of the hippocampus, as assessed using the watermaze DMP task. However, $MnCl_2$ injection induced some acute side effects (severe ataxia, erythema) subsiding within 30 min, as well as some skin irritation at the injection site and weight reduction.

4.1. No effects of $MnCl_2$ on hippocampus-dependent behavioral performance

The DMP task, requiring adaptive behavior based on rapid place learning, is a very sensitive assay of normal hippocampal function, and studies in our laboratory have previously shown that a range of hippocampal manipulations, including small partial hippocampal lesions and infusions of drugs that interfere with hippocampal plasticity mechanisms, result in pronounced performance deficits [26–29]. Thus, the absence of any impairment in performance measures on the DMP task following injection of 200 μmol/kg $MnCl_2$ indicates that the resulting Mn^{2+} accumulation within the hippocampus does not interfere strongly with hippocampal function, even though peripheral side effects of the injection (see Section 4.2) may interfere with performance on hippocampus-dependent tasks relying on food-motivated or spontaneous behavior.

Our new findings in Lister hooded rats are consistent with a very recent study in Sprague–Dawley rats [14]. This study demonstrated that 100 or 500 μmol/kg $MnCl_2$ did not cause any gross histopathological signs of neurotoxicity within the hippocampus and interfered only minimally with hippocampal synaptic transmission and plasticity (only a small reduction in excitatory transmission at enthorinal-dentate gyrus synapses at 500 μmol/kg, suggested to reflect pre-synaptic Ca^{2+} antagonism) and with hippocampus-dependent behavior on a food-reinforced T-maze alternation task (only an increase in response latencies, without reduction in choice accuracy, at 500 μmol/kg).

4.2. Peripheral non-specific side effects of $MnCl_2$

Injection of $MnCl_2$ into the peritoneum caused virtually immediate severe ataxia, which appeared to be due to loss of abdominal muscle control. This may have been caused by acute Mn^{2+} overexposure interfering with Ca^{2+} signaling necessary for proper muscle function [20,37]. The acute erythema observed immediately after $MnCl_2$ injection is consistent with the vasodilatory properties [38] of $MnCl_2$ and the "flushing" in human patients following administration of a Mn^{2+} based MR contrast agent [20]. Both acute effects appeared to have subsided within around 30 min, so would not interfere much with any cognitive testing. These acute effects are also unlikely to interfere much with the use of MEMRI to map behavior-related regional brain activation, as they would have subsided by the time substantial amounts of Mn^{2+} have entered the

extracellular space of brain regions protected by a blood–brain barrier (1–2 h following systemic $MnCl_2$ administration), i.e. when the time window for behavior-related neuronal Mn^{2+} uptake (which can later be measured by MEMRI) begins in these regions [1,9,13,14,31,39]. The normal swimming and platform behavior in the watermaze 1–2 h and 24 h after $MnCl_2$ injection corroborates that 200 μmol/kg $MnCl_2$ did not interfere strongly with sensorimotor function, apart from temporary acute effects. It should be noted, though, that one recent study found that voluntary wheel running behavior in Sprague–Dawley rats was reduced for around 1 day after injection of 200 μmol/kg $MnCl_2$ and for more than 2 days after injection of 500 μmol/kg [6]. It is possible that, in the watermaze, the rats' strong motivation to escape from water compensates for minor impairments in motor behavior that may be detected in situations involving spontaneous movement.

The weight loss of rats injected with $MnCl_2$ and the fact that these rats did not reach the normal weight–growth curve of control rats within the 16 days monitored, however, indicate that acute Mn^{2+} administration can have long-lasting adverse effects on the rats' physiology. This is consistent with previous reports of weight loss in Sprague–Dawley rats following injections of $MnCl_2$ at doses similar to or higher than in our study [6,21]. The mechanisms underlying these effects are not clear, but the weight effects of Mn^{2+} may reflect a broad interference with normal physiological processes [20].

4.3. Conclusion

Our data support the notion that hippocampal function is not substantially impaired by hippocampal Mn^{2+} accumulation that produces pronounced hippocampal MR signal enhancement (also see [14]). Thus, combination of MEMRI with cognitive testing remains a viable strategy for the study of hippocampal function in rodent models. However, if systemic administration of 200 μmol/kg $MnCl_2$, as examined in the present study, will enable 'functional mapping', i.e. the detection of behavior-related regional brain activation, using MEMRI remains to be clarified (for a good discussion of issues to be considered for functional mapping by MEMRI, see [6]). Moreover, attention must be paid to adverse peripheral side effects. Such effects interfere with animal welfare and may confound research involving MEMRI, depending on the study type. For example, the adverse effects of Mn^{2+} on normal peripheral physiological processes may be exacerbated in longitudinal studies involving cumulative Mn^{2+} exposure or animal models with pre-existing impairments. Recently introduced slow Mn^{2+} administration via implanted osmotic minipumps [40] can minimize peripheral side effects due to acute Mn^{2+} overexposure, even though this method did not totally prevent the interference of Mn^{2+} with normal weight growth [6]; sufficient 'fractionation' of $MnCl_2$ injections may yield similar results [21]. Direct administration of Mn^{2+} into the brain, using intra-cerebroventricular or intracerebral microinfusion [8,9,41], may circumvent any peripheral side effects, but at the expense of requiring invasive stereotaxic surgery.

Acknowledgements

We thank Patrick Spooner for software and technical support, Ann Paterson for assistance with the behavioral testing, Richard Watson for animal care and help with injections, Jane Gebbie and Carolyn Quigley for veterinary support, Marie Pezze for comments on an earlier version of the manuscript, and Richard Morris for his encouragement of these studies, for discussions and for providing behavioral testing facilities. This work was financed by a Caledonian Research Foundation Personal Fellowship, a pilot grant from the MRI endowment funds and Neuroscience Honours project bench fees (College of Medicine and Veterinary Medicine, University of Edinburgh) to T.B. and a RCUK Academic Fellowship to J.Y. A.M. was supported by an MRC Clinician Scientist Fellowship. The preclinical 7-T MRI scanner and MRI equipment were acquired with a grant from the British Heart Foundation to Keith Fox (Second Cardiovascular Initiative).

References

[1] Silva AC, Lee JH, Aoki I, Koretsky AP. Manganese-enhanced magnetic resonance imaging (MEMRI): methodological and practical considerations. NMR Biomed 2004;17:532–43.
[2] Lin YJ, Koretsky AP. Manganese ion enhances T1-weighted MRI during brain activation: an approach to direct imaging of brain function. Magn Reson Med 1997;38:378–88.
[3] Chen W, Tenney J, Kulkarni P, King JA. Imaging unconditioned fear response with manganese-enhanced MRI (MEMRI). Neuroimage 2007;37:221–9.
[4] Bissig D, Berkowitz BA. Manganese-enhanced MRI of layer-specific activity in the visual cortex from awake and free-moving rats. Neuroimage 2009;44:627–35.
[5] Chuang KH, Lee JH, Silva AC, Belluscio L, Koretsky AP. Manganese enhanced MRI reveals functional circuitry in response to odorant stimuli. Neuroimage 2009;44:363–72.
[6] Eschenko O, Canals S, Simanova I, Beyerlein M, Murayama Y, Logothetis NK. Mapping of functional brain activity in freely behaving rats during voluntary running using manganese-enhanced MRI: implication for longitudinal studies. Neuroimage 2010;49:2544–55.
[7] Kuo YT, Herlihy AH, So PW, Bell JD. Manganese-enhanced magnetic resonance imaging (MEMRI) without compromise of the blood–brain barrier detects hypothalamic neuronal activity in vivo. NMR Biomed 2006;19:1028–34.
[8] Watanabe T, Radulovic J, Boretius S, Frahm J, Michaelis T. Mapping of the habenulo-interpeduncular pathway in living mice using manganese-enhanced 3D MRI. Magn Reson Imaging 2006;24:209–15.
[9] Watanabe T, Frahm J, Michaelis T. Functional mapping of neural pathways in rodent brain in vivo using manganese-enhanced three-dimensional magnetic resonance imaging. NMR Biomed 2004;17:554–68.
[10] Yu X, Wadghiri YZ, Sanes DH, Turnbull DH. In vivo auditory brain mapping in mice with Mn-enhanced MRI. Nat Neurosci 2005;8:961–8.
[11] Andersen PMR, Amaral D, Bliss T, O'Keefe J. The hippocampus book. Oxford: Oxford University Press; 2007.
[12] Bast T. Toward an integrative perspective on hippocampal function: from the rapid encoding of experience to adaptive behavior. Rev Neurosci 2007;18:253–81.
[13] Aoki I, Wu YJ, Silva AC, Lynch RM, Koretsky AP. In vivo detection of neuroarchitecture in the rodent brain using manganese-enhanced MRI. Neuroimage 2004;22:1046–59.
[14] Eschenko O, Canals S, Simanova I, Logothetis NK. Behavioral, electrophysiological and histopathological consequences of systemic manganese administration in MEMRI. Magn Reson Imaging 2010. Epub ahead of print.
[15] Fone KC, Porkess MV. Behavioural and neurochemical effects of post-weaning social isolation in rodents-relevance to developmental neuropsychiatric disorders. Neurosci Biobehav Rev 2008;32:1087–102.
[16] Hibberd C, Yau JL, Seckl JR. Glucocorticoids and the ageing hippocampus. J Anat 2000;197(Pt 4):553–62.
[17] Lodge DJ, Grace AA. Gestational methylazoxymethanol acetate administration: a developmental disruption model of schizophrenia. Behav Brain Res 2009;204:306–12.
[18] Meyer U, Feldon J. Neural basis of psychosis-related behaviour in the infection model of schizophrenia. Behav Brain Res 2009;204:322–34.
[19] Morris RG. Episodic-like memory in animals: psychological criteria, neural mechanisms and the value of episodic-like tasks to investigate animal models of neurodegenerative disease. Philos Trans R Soc Lond B: Biol Sci 2001;356:1453–65.
[20] Crossgrove J, Zheng W. Manganese toxicity upon overexposure. NMR Biomed 2004;17:544–53.
[21] Bock NA, Paiva FF, Silva AC. Fractionated manganese-enhanced MRI. NMR Biomed 2008;21:473.
[22] Takeda A. Manganese action in brain function. Brain Res Rev 2003;41:79–87.
[23] Guilarte TR, Chen MK. Manganese inhibits NMDA receptor channel function: implications to psychiatric and cognitive effects. Neurotoxicology 2007;28:1147–52.
[24] Berkowitz BA, Roberts R, Goebel DJ, Luan H. Noninvasive and simultaneous imaging of layer-specific retinal functional adaptation by manganese-enhanced MRI. Invest Ophthalmol Vis Sci 2006;47:2668–74.
[25] Berkowitz BA, Roberts R, Luan H, Bissig D, Bui BV, Gradianu M, et al. Manganese-enhanced MRI studies of alterations of intraretinal ion demand in models of ocular injury. Invest Ophthalmol Vis Sci 2007;48:3796–804.
[26] Steele RJ, Morris RGM. Delay-dependent impairment of a matching-to-place task with chronic and intrahippocampal infusion of the NMDA-antagonist D-AP 5. Hippocampus 1999;9:118–36.
[27] de Hoz L, Moser EI, Morris RG. Spatial learning with unilateral and bilateral hippocampal networks. Eur J Neurosci 2005;22:745–54.

[28] O'Carroll CM, Martin SJ, Sandin J, Frenguelli B, Morris RGM. Dopaminergic modulation of the persistence of one-trial hippocampus-dependent memory. Learn Memory 2006;13:760.
[29] Bast T, Wilson IA, Witter MP, Morris RGM. From rapid place learning to behavioral performance: a key role for the intermediate hippocampus. PLoS Biol 2009;7:730–46.
[30] Yau JL, Noble J, Kenyon CJ, Hibberd C, Kotelevtsev Y, Mullins JJ, et al. Lack of tissue glucocorticoid reactivation in 11beta -hydroxysteroid dehydrogenase type 1 knockout mice ameliorates age-related learning impairments. Proc Natl Acad Sci USA 2001;98:4716–21.
[31] Tambalo S, Daducci A, Fiorini S, Boschi F, Mariani M, Marinone M, et al. Experimental protocol for activation-induced manganese-enhanced MRI (AIM-MRI) based on quantitative determination of Mn content in rat brain by fast T1 mapping. Magn Reson Med 2009;62:1080–4.
[32] Spooner RIW, Thomson A, Hall J, Morris RGM, Salter SH. The Atlantis platform: a new design and further developments of Buresova's on-demand platform for the water maze. Learn Memory 1994;1:203–11.
[33] Faul F, Erdfelder E, Lang AG, Buchner A. G*Power 3: a flexible statistical power analysis program for the social, behavioral, and biomedical sciences. Behav Res Methods 2007;39:175–91.
[34] Ahlander M, Misane I, Schott PA, Ogren SO. A behavioral analysis of the spatial learning deficit induced by the NMDA receptor antagonist MK-801 (dizocilpine) in the rat. Neuropsychopharmacology 1999;21:414–26.
[35] Cain DP, Saucier D, Boon F. Testing hypotheses of spatial learning: the role of NMDA receptors and NMDA-mediated long-term potentiation. Behav Brain Res 1997;84:179–93.
[36] Morris RG. Synaptic plasticity and learning: selective impairment of learning rats and blockade of long-term potentiation in vivo by the N-methyl-D-aspartate receptor antagonist AP5. J Neurosci 1989;9:3040–57.
[37] Chiarandini DJ, Stefani E. Effects of manganese on the electrical and mechanical properties of frog skeletal muscle fibres. J Physiol 1973;232:129.
[38] Kasten TP, Settle SL, Misko TP, Currie MG, Nickols GA. Manganese potentiation of nitric oxide-mediated vascular relaxation. Eur J Pharmacol 1994;253:35–44.
[39] Lee JH, Silva AC, Merkle H, Koretsky AP. Manganese-enhanced magnetic resonance imaging of mouse brain after systemic administration of $MnCl_2$: dose-dependent and temporal evolution of T1 contrast. Magn Reson Med 2005;53:640–8.
[40] Canals S, Beyerlein M, Keller AL, Murayama Y, Logothetis NK. Magnetic resonance imaging of cortical connectivity in vivo. Neuroimage 2008;40:458–72.
[41] Nairismagi J, Pitkanen A, Narkilahti S, Huttunen J, Kauppinen RA, Grohn OH. Manganese-enhanced magnetic resonance imaging of mossy fiber plasticity in vivo. Neuroimage 2006;30:130–5.